INFERENCES ON CORONAL MAGNETIC FIELDS FROM SOHO UVCS OBSERVATIONS

G. POLETTO
Osservatorio Astrofisico di Arcetri,
Largo Enrico Fermi, 5, 50125 Firenze, Italy

M. ROMOLI
Dipartimento di Astronomia e Scienza dello Spazio,
Università di Firenze, Italy

S. T. SUESS
NASA Marshall Space Flight Center, SSL/ES82,
Huntsville, AL 35812, USA

and

A. H. WANG and S. T. WU
Center for Space Plasma and Aeronomic Research,
The University of Alabama, Huntsville, USA

Abstract. The characteristics of the magnetic field ubiquitously permeating the coronal plasma are still largely unknown. In this paper we analyze some aspects of coronal physics, related to the magnetic field behavior, which forthcoming SOHO UVCS observations can help better understand. To this end, three coronal structures will be examined: streamers, coronal mass ejections (CMEs) and coronal holes.

As to streamers and CMEs, we show, via simulations of the Ly-α and white light emission from these objects, calculated on the basis of recent theoretical models (Wang et al., 1995), how new data from SOHO can help advancing our knowledge of the streamer/CME magnetic configuration. Our discussion highlights also those observational signatures which might offer clues on reconnection processes in streamers' current sheets.

Coronal holes (CHs) are discussed in the last section of the paper. Little is known about CH flux tube geometry, which is closely related to the behavior of the solar wind at small heliocentric distances.

Indirect evidence for the flux tube spreading factors, within a few solar radii, is here examined.

Key words: Solar Corona – CME – UV Spectroscopy

1. Introduction

The Ultraviolet Coronagraph Spectrometer (UVCS) onboard SoHO is designed for ultraviolet spectroscopy and visible light polarimetry of the solar corona. The experiment and its primary scientific objectives have been described by Kohl et al. (1995): because the instrument has the capability of observing the solar corona from $\approx$ 1.2 to 10 R_{sun}, we expect UVCS to yield a wealth of data, crucial to our understanding of the source regions of the solar wind, of its acceleration processes, and, more generally, of the processes by which the corona is being heated. However, although being not devised

for this purpose, UVCS can also contribute to our knowledge of coronal magnetic fields, by means of indirect measurements.

In the context of this meeting, it is especially interesting to investigate how UVCS provides information on magnetic field-related issues, as an example of the additional knowledge that complements direct magnetic field measurements and/or theoretical predictions. For illustrative purposes, in the following sections we consider, separately, streamers, coronal mass ejections (CMEs) and coronal holes, to represent structures/phenoema typical of the quiet and active corona. For each of them, we describe the data UVCS can acquire and analyze how the provided information help us building a better scenario for the behavior of magnetic fields in the extended solar corona.

2. Magnetic field in streamers

There are at least two distinct measurements that UVCS can make, which are relevant to the magnetic field behavior in streamers: the following two sub-sections deal with these separately.

2.1 3-D STREAMERS' STRUCTURE

Streamers, observed now for many decades, in eclipse and/or with coronagraphic techniques, appear as bright large-scale features which extend out to heliocentric distances of the order of a few R_{sun}. Because they are seen in projection onto the plane of the sky, little is known about their 3-D structure, and we can't say when, possibly depending on the solar activity cycle, they form a continuous belt which circles the Sun, or when they are isolated, distinct features. In order to identify their spatial structure, we can resort either to a detailed comparison between observations and fictitious data reconstructed after integrating over parameters from 3-D theoretical models, or make use of available measurements to derive, via appropriate techniques, the original 3-D configuration. It is beyond the scope of the present paper to review theoretical models; hence, it will suffice to remind readers that 3-D streamer models are still scanty and not sophisticated enough to allow for a meaningful comparison with observational data (see, e.g., Wu and Wang, 1991; Bagenal and Wilson, 1991; Cuperman, et al., 1993).

The spatial structure of streamers can be derived via tomographic techniques, provided these objects, carried around by solar rotation, are observed over a time interval long enough. Streamers are most commonly observed in white light and their polarization brightness (pB) is proportional to the line-of-sight (LOS) integral of the electron density (times a scattering function). A number of algorithms (analytic inversion, Fourier Transform, algebraic reconstruction techniques) yield, from a pB observational set acquired over a few days, the 3-D distribution of density within the structure. This kind

of work has never been popular: although recently Aschwanden and Bastian (1994a, 1994b) investigated the active region behavior at radio wavelengths via VLA stereoscopy, the streamer 3-D shape has been derived by means of this technique only in a PhD thesis by Wilson (1977). Most probably, reconstruction techniques based on prolonged observations of features met with limited consensus because temporal and spatial variations within the structure cannot be easily separated. Obviously, simultaneous observations from multiple vantage points are free from such criticisms (Davila, 1993; Batchelor, 1994; Schmidt and Bothmer, 1996).

In the context of the present paper, we are interested in reconstruction techniques only as a means to determine the overall streamer configuration – i. e. the overall field morphology – identified by the streamer 3-D density distribution. Streamers' images can be constructed in white light, with LASCO (or, possibly, with the UVCS White Light Channel) as well as in Ly-α and other lines. In order to get some more insight into the capabilities of the technique, we have simulated the Ly-α intensity from a streamer, at different heliocentric altitudes, for different position angles α of the structure with respect to the plane of the sky. To this end, we adopted the 2-D streamer models of Wang et al. (1995), and calculated the distribution of the Ly-α emissivity ($erg\ cm^{-3}\ s^{-1}\ sr^{-1}$) along the LOS. We refer the reader to Wang et al. (1995) for a description of the physical characteristics of the streamer models: for the calculation of the Ly-α emissivities we consider a scenario where both the dipolar streamer and the LOS lie onto the sun equatorial plane, at zero heliographic latitude, and the LOS is normal to the plane of the sky. Although is probably unrealistic to assume the streamer's footpoints to be located at the same latitude, our assumption is in the present case justifiable, inasmuch we consider the 2-D plane to constitute a section of a 3-D structure, whose extension, in the third dimension, is not specified.

We remind the reader that the total (i. e. integrated over the the line profile) Ly-α intensity, as observed along the LOS direction $\mathbf{n}$ is given by (Kohl and Withbroe, 1982)

$$I = \frac{hB_{12}\lambda_0}{4\pi} \int_{-\infty}^{\infty} N_1 dx \int_{\Omega} p(\varphi) d\omega' \int_0^{\infty} I_{chrom}(\lambda, \mathbf{n}') \Phi(\lambda - \lambda_0) d\lambda \quad (1)$$

where h is the Planck constant; B_{12} the Einstein coefficient for the line; λ_0 is the rest value for the central wavelength λ of the Ly-α transition; N_1 is the number density of hydrogen atoms in the ground level; the unit vector $\mathbf{n}$ is along the line of sight x and the unit vector $\mathbf{n}'$ is along the direction of the incident radiation; φ is the angle between $\mathbf{n}$ and $\mathbf{n}'$; $p(\varphi)\ d\omega'$ -where ω' is the solid angle around $\mathbf{n}'$- is the probability that a photon travelling along the direction $\mathbf{n}$ was travelling, before scattering, along the direction $\mathbf{n}'$; Ω is the solid angle subtended by the chromosphere at the point of scattering; I_{chrom} is the exciting chromospheric radiation and Φ

is the coronal absorption profile. In our calculations we assume that the intensity of the chromospheric Ly-α radiation is constant across the solar disk and that the velocity distribution of the scattering hydrogen atoms is Maxwellian. The expression for the dependence of the Ly-α scattering process on the angle has been taken from Beckers and Chipman (1974) and we adopted the values given by Gabriel (1971) for the ratio between the neutral hydrogen density and the proton density at different temperatures (because of the low coronal density all hydrogen atoms are assumed to be in the ground level, therefore $\frac{N_H}{N_p} = \frac{N_1}{N_p}$).

Figure 1 shows the percentage contribution to the total Ly-α intensity of volume elements located along the line of sight, for different position angle of the streamer. When the streamer axis is in the plane of the sky ($\alpha = 0$), the LOS is normal to the axis and, quite obviously, the main contribution to the Ly-α intensity originates from the volume element which is, along the LOS, closest to the Sun and lies on the streamer's axis. However, when $\alpha \neq 0$, the closest element to the Sun, along a LOS through the streamer, may lie at some distance from the streamer axis, and, depending on the density distribution *across* the streamer, with respect to the density distribution *along* the streamer, the possibility arises of deriving some information about the density profile across the streamer.

Figure 1 shows, for a polytropic streamer ($\gamma = 1.05$, see Wang et al. model 2), the distribution of the Ly-α emissivities along the LOS as a function of the distance from the streamer axis. On the vertical axis the percentage contribution to the total Lyman intensity originating from different volume elements is given: panels refer to streamers at different position angles with respect to the plane of the sky. For $\alpha = 52°$, a contribution of only 5-6% to the Ly-α intensity comes from plasma at the streamer's axis, while a 60% contribution, originates from elements at a distance of 1.5 R_{sun} from the streamer axis.

As we anticipated, this technique may be questioned on the basis of the temporal variability of the structures. Moreover, further difficulties are met whenever discrete structures lie along the LOS: however, if sufficiently apart, it may become possible to identify them as separate objects. Hence, in spite of these limitations, it is worth pursuing this line of research to have some indications about the streamer magnetic field morphology and, possibly, to understand whether the equatorial belt is made up of discrete features or of a continuous structure.

2.2 Current sheet in streamers

The closed field configuration of streamers is surrounded by open fields: curved current sheets separating closed and open regions merge into a single sheet at the streamer's "cusp". Order of magnitude estimates for the values of the physical parameters in the current sheet above the top of closed loops

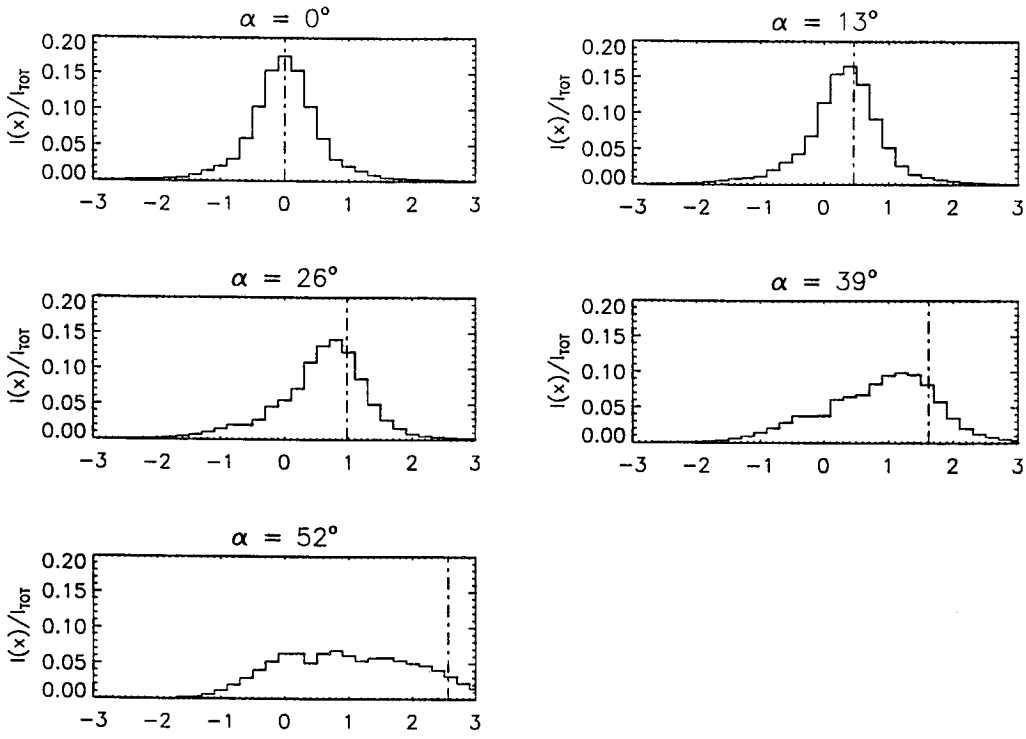

Fig. 1. Distribution of the $Ly-\alpha$ emissivities along the line of sight for a streamer at different position angles α with respect to the plane of the sky. The emissivities have been computed on the basis of a streamer model by Wang et al. (1995); on the vertical axis the percentage contribution of the emissivity originating at different distances from the streamer axis is given. Distances from the streamer axis (in units of R_{sun}) are shown in the abscissa. The dashed bar gives the distance, measured from the plane of the sky, at which the line of sight intersects the streamer's axis. In all panels, the line of sight is assumed to intersect the plane of the sky at a heliocentric distance of 2 R_{sun}.

have been derived by Pneuman (1982), who gives density and temperature of the order, respectively, of $10^9\ cm^{-3}$ and $10^6\ K$, and radial magnetic field strength of $\approx .5\ G$ and a transverse field of $\approx 2 \times 10^{-3}\ G$. The thickness of the sheet has been evaluated to be of the order of a few hundreds kilometers. Processes occurring in the cusp area are hardly known and may depend on the mechanism of formation of streamers: be it the progressive filling, by ascending plasma, of large scale closed structures, outwardly stretched, or the ongoing reconnection of open fields. Observational evidence for reconnection phenomena at the streamer top could solve this ambiguity and UVCS may be capable of identifying signatures of reconnection processes.

Somov (1992) has developed a model for magnetic reconnection in a high temperature turbulent current sheet (HTTCS), where plasma entering the

sheet is ejected in opposite direction, along the sheet, at a velocity (on the order of the Alfvèn speed), which is a function of the electron temperature, of the electron-to-ion temperature ratio and of the mean molecular weight of the plasma within the sheet. Observational signatures for these outflows can be provided by symmetric, non-thermal broadenings of spectral lines: Antonucci and Somov (1996) and Antonucci et al. (1996), analyzing the profiles of X-ray lines acquired by the Bent Crystal Spectrometer (BCS) on SMM during solar flares, found them to be consistent with predictions from the HTTCS model.

Non-thermal broadenings of UV lines observed by UVCS can analogously expected to be a clue for the presence of reconnection processes in the cusp area. However, non thermal symmetric broadenings at coronal heights allow for different interpretations as well: because, in order to interpret them in terms of reconnection, one should be able to rule out the presence of plasma, in the fore and background, giving rise to similar broadenings. Being the streamer cusp immersed in a steadily expanding solar wind plasma, it may be difficult to draw definite conclusions. Moreover the timing factor, which is crucial in flare analysis, where it helps establish a causal relationship between different phenomena, is missing in streamers observations, because we expect reconnection to go on continuously in the cusp area.

Alternately, it has been suggested that magnetic islands, formed by tearing instability in the current sheet, could be observable and thus constitute a further signature of reconnection processes. Verneta et al. (1994) and Dahlburg and Karpen (1995), predicted the emission measures from such islands and the growth times for the instability. Verneta et al. estimate emission measure values $\leq 10^{47}\ cm^{-3}$, for elongated ($\approx 2 \times 10^{10}\ cm$) plasmoids, with a $\approx$ 10 hour lifetime, drifting outwards at a speed increasing from $.4\ km\ s^{-1}$ to $40\ km\ s^{-1}$ over the 2 to 4 R_{sun} distance. Assuming the current sheet to lie along the LOS, Verneta et al. claim the intensities of OVI, MgX, Fe XII, Si XII lines to be strong enough to be easily observable by UVCS.

Similar conclusions have been reached by Dahlburg and Karpen (1995), who developed a model for a triple current sheet formed by two neighboring helmet streamers. These authors conclude that the magnetic topology of adjacent streamers is subject to instabilities, with growth times of the order of hours, and predict the formation of plasmoids with emission measures on the order of $10^{44} - 10^{46}\ cm^{-3}$. Because these authors don't give any estimate of the lifetime and propagation speed of the magnetic islands, is difficult to estimate their detectability. In conclusion, although we may find evidence for magnetic reconnection analyzing processes occurring in the streamer cusp/current sheet areas, the interpretation of the outlined measurements is not obvious. Most likely, observations will provide consistency arguments, rather than an uncontroversial proof for the occurrence of reconnection.

3. The magnetic configuration of coronal mass ejections.

As for streamers, the visual appearance of coronal mass ejections (CMEs) depends on the spatial distribution of electrons along the LOS and we perceive only the projection onto the plane of the sky of their 3-D spatial structure. The latter is relevant, not only *per se*, but also because is thought to be related to the CME acceleration mechanism (Anzer, 1978; Muschovias and Poland, 1978; Dryer, 1982). Because CMEs' lifetime is of the order of a few hours, their 3-D structure cannot be identified via observations at different angles with respect to the plane of the sky, as described in the previous section. Nevertheless, tomographic techniques have allowed Jackson and Froehling (1995) to reconstruct the 3-D density distribution of a CME in the interplanetary medium from data acquired by Helios and Solwind experiments. The CME turned out to consist of two lobes of material, in a shape not fitting the CME standard morphologies. Many authors made classification schemes based on the visual appearance of CMEs (see, e.g., Hundhausen, 1996, and references within): although not entirely consistent, these authors agree considering loop-like, isolated amorphous blobs and mounds among the most common configurations.

In the following, we focus on these categories, to examine whether UVCS observations can contribute to the understanding of the relationship between their visual appearance and their magnetic field configuration. To this end, we made simulations of the white light and Ly-α emission from loop-like, plasmoids and mounds, on the basis of two dimensional models worked out by Wang et al. (1995), who give the physical parameters and magnetic configuration of these structures at different times during the CME evolution. Loop-like CMEs and mounds are similar structures, but they differ because of the different shape of their fieldlines, which, although never forming a detached plasmoid, as it happens for blobs, are either stretched out in the radial direction to form, in mounds, sort of a spike, or, in loop-like CMEs, expand laterally (azimuthally) in their upper parts, as CMEs propagate upwards through the corona. In the initial phase of evolution, also blobs are anchored to the coronal base, and it is thus difficult to recognize the different configurations.

In Figure 2 we show the percentage increase, over their pre-event value, of the white light and Ly-α intensity from these three kind of CMEs, calculated on the basis of Wang's et al. predictions. For these simulations, we assumed the line of sight to be normal to the direction of propagation of the CME, which lies on the plane of the sky. We further assumed that Wang et al. computational plane contains the LOS and the direction of propagation of the CME, thus we choose the worst possible scenario, as far as the identification of these structures is concerned, as they would be seen edge-on.

Figure 2 shows that, whereas the white light emission from CMEs is

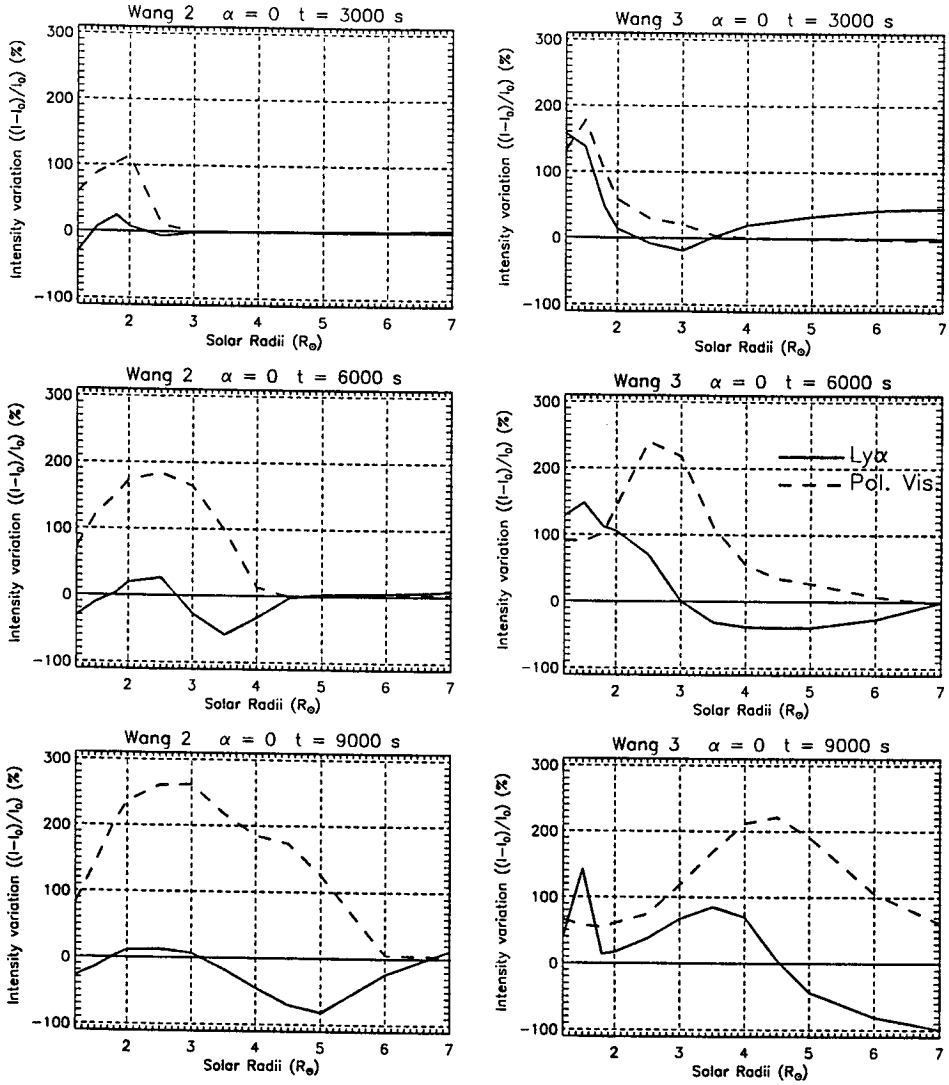

Fig. 2. Percentage intensity variation, with respect to the pre-event atmosphere, in white light (dashed line) and $Ly-\alpha$ (solid line) radiation, at different times during a coronal mass ejection, as a function of the heliocentric distance. Simulations have been made on the basis of Wang et al. (1995) loop-like and blob CMEs (labeled, respectively, Wang 2 and 3).

always greater than the pre-event emission, the CMEs signature in Ly-α is a *decrease* of intensity. White light observations, if not complemented by additional data, would hardly permit mounds or loop-type CMEs to be distinguishable from blob CMEs, at least within the first 3-4 solar radii. However, if we focus on model results at 6000 s after the CME initiation, it is apparent that the Ly-α intensity for a plasmoid centered at 2-3 R_{sun},

is 50% lower than its pre-event value all over the atmosphere *ahead* of the plasmoid, while this effect is limited to a small height interval for the loop-like feature. The Ly-α intensity decrease is due to the Doppler dimming of the line, caused by the plasma expansion speed: Wang et al. model predicts the whole atmosphere ahead of the blob CME to be expanding, contrary to what happens for a loop structure. It's worth pointing out that mounds as well are preceded by an expanding plasma: however, their peak emission, both in white light and in Ly-α, does not shift with time to higher distances, as shown by the other two types of CMEs.

The above stated conclusions could be questioned as being model-dependent. This criticism can't be dismissed, even if there are indications, from 3-D simulations of coronal mass ejections (Steinolfson, 1992), that 3-D numerical solutions in a meridional plane are very similar to those resulting from 2-D simulations. Hence, although aware of the limitations implicit in results from numerical modeling, we may conclude that, at least qualitatively, coupled white light and Ly-α observations have the capability of identifying the magnetic structure of CMEs, *provided data are taken over an extended range of distances.*

4. The magnetic configuration of coronal holes.

High speed solar wind streams have been recognized to originate from coronal holes, where field lines, open towards the interplanetary space, are rooted. On the contrary, the source regions of the slow wind are little known, so far. although the upper sections of streamers, where field lines open up, are considered as likely candidates. Independent of the wind speed, it is generally assumed that magnetic fields, and their geometry, play an essential role in determining the wind characteristics: in a pioneering work Kopp and Holzer (1976) demonstrated that the flow topology depends on the flow tubes expansion factor *f(r)* (where the *expansion factor f(r)* is defined by the relationship $A(r) = A(R_{sun})(r/R_{sun})^2 f(r)$, A(r) being the flow tube area at the heliocentric distance r). In particular, high $f(r)$ imply low densities and supersonic speeds at low heliocentric altitudes (although Kopp and Holzer asymptotic flow speeds are independent of the expansion factor).

From the observational side, Munro and Jackson (1977) found the cross-sectional area of a polar coronal hole observed by Skylab to increase, between 1 and 3 R_{sun}, by a factor seven: that is, more rapidly than implied by a radial expansion, but less rapidly than predicted by potential field calculations (Levine et al., 1977). Wang and Sheeley have, more recently, studied the correlation between solar wind speeds and expansion factors – the latter evaluated from source surface model techniques – and found an inverse correlation between solar wind speed, measured at 1 A.U., and coronal expansion factors (Wang and Sheeley, 1990). These two works are not

in contrast, because Wang and Sheeley analyzed the behavior of individual flux tubes, rather than of the overall coronal hole region, and came to the conclusion that, within a hole, the fastest wind should originate from mid-latitude coronal hole extension (Wang and Sheeley, 1994): a prediction, however, so far not confirmed by Ulysses high latitude observations (Phillips et al., 1995).

Obviously, a determination of the wind speed and/or spreading factors, at low heliocentric distances, would constitute a crucial data, in a field where a unified scenario has not yet been reached. UVCS, via the Doppler dimming technique, can measure the wind speed at distances of the order of a few solar radii, thus providing first-hand evidence for the magnetic field geometry within coronal holes. Because the $Ly-\alpha$ and OVI lines, observed by UVCS, in the extended corona are produced by resonantly scattered disk radiation, they reach maximum intensity when the plasma has zero outflow velocity: an outflow speed, as expected in coronal holes, however, *Doppler dims* the lines, because the scattering hydrogen atoms see a red-shifted incident disk radiation. As a result, the outflowing plasma emission is drastically reduced and may even disappear, when the disk radiation shifts off the coronal line. This phenomenon allows one to evaluate the outflow plasma speed, when densities and temperatures are known, by finding the velocity profile capable of reproducing the observed line intensities.

This technique has already been used by Strachan (1990), who found data $Ly-\alpha$ data from rocket flights to be consistent with supersonic speeds of coronal hole plasma at a heliocentric distance as low as $\approx 2\ R_{sun}$. Such high speeds point to a high expansion factor of the coronal hole magnetic field, although measurement are not accurate enough to allow its precise determination ($f(r)$ values in the range 3-7 are compatible with data). Further applications of this technique are left to UVCS, which appears capable of advancing our knowledge of the magnetic field geometry in regions so far unexplored. In my opinion, this research area is especially intriguing and will provide researcher in wind theories, and magnetic field modellers, with new, invaluable data.

5. Conclusions

We have here presented a number of observations, to be performed by SoHO UVCS, which have a bearing on the magnetic field behavior in various coronal structures. UVCS can help determining the 3-D streamer configuration (establishing the morphology of regions with selected physical conditions, like high temperatures/velocities) and the location and physical characteristics of the helmet streamers current sheets; can provide information about the topology of coronal mass ejections; can yield crucial data about the magnetic field spreading factor within coronal holes. We deem it imperative to

check such indirect magnetic field knowledge vs. theoretical magnetic field extrapolations, in order to get a realistic scenario of the magnetic field behavior at coronal levels: this is one of the areas where we expect the SoHO mission to bring major advancements.

Acknowledgements

The work of G. Poletto and M. Romoli has been partially supported by ASI (Italian Space Agency). M. Romoli acknowledges partial support also from SAO. S. T. Suess acknowledges support from the NASA Ulysses project. A.-H. Wang and S. T. Wu are partially supported by ~~NASA~~ NSF Grant ATM 9215673.

References

Anzer, U.: 1978, *Solar Phys.* **57**, 111
Antonucci, E., Somov, B.: 1996, *Astrophys. J.* **456**, 833
Antonucci, E., Benna, C., Dodero, M. A., Martin, R.: 1996, *Adv. Space Res.* **17**, 47
Aschwanden, M. J., Bastian, T. S.: 1994a, *Astrophys. J.* **426**, 425
Aschwanden, M. J., Bastian, T. S.: 1994b, *Astrophys. J.* **426**, 434
Bagenal, F., Gibson, S.: 1991, *J. Geophys. Res.* **96**, 17663
Batchelor, D.: 1994, *Solar Phys.* **155**, 57
Cuperman, S., Bruma, C., Detman, T. R., Dryer, M.: 1993, *Astrophys. J.* **404**, 356
Dahlburg, R. B., Karpen, J. T.: 1995, *J. Geophys. Res.* **100**, 23489
Davila, J. M.: 1993, *Solar Tomography*, NASA GSFC report
Dryer, M.: 1982, *Space Sci. Rev* **33**, 233
Hundhausen, A. J.: 1996, 'A Summary of SMM Observations' in K. Strong, ed(s)., *The Many Faces of the Sun*, in press,
Jackson, B. V., Froehling, H. R.: 1995, *Astron. Astrophys.* **299**, 885
Kohl, J.L, Esser, R., Gardner, L.D., Habbal, S., Daigneau, P.S., Dennis, E.F., Nystrom, G.U., Panasyuk, A., Raymond, J.C., Smith, P.L., Strachan, L., van Ballegooijen, A.A., Noci, G., Fineschi, S., Romoli, M., Ciaravella, A., Modigliani, A., Huber, M.C.E., Antonucci, E., Benna, C., Giordano, S., Tondello, G., Nicolosi, P., Naletto, G., Pernechele, C., Spadaro, D., Poletto, G., Livi, S., von der Lühe, O., Geiss, J., Timothy, J.G., Gloeckler, G., Allegra, A., Basile, G., Brusa, R., Wood, B., Siegmund, O.H.W., Fowler, W., Fisher, R., Jhabvala, M.: 1995, *Solar Phys.* **162**, 313
Kohl, J. L., Withbroe, G. L.: 1982, *Astrophys. J.* **256**, 263
Kopp, R. A., Holzer, T. E.: 1976, *Solar Phys.* **49**, 212
Levine, R., Altschuler, M., Harvey, J. W., Jackson, B. V.: 1977, *Astrophys. J.* **215**, 636
Munro, R. H., Jackson, B. V.: 1977, *Astrophys. J.* **213**, 874
Muschovias, T., Poland, A. I.: 1978, *Astrophys. J.* **110**, 115
Phillips, J.L., Bame, S.J., Feldman, W.C., Gosling, J.T., Hammond, C.M., McComas, D.J., Goldstein, B.E., Neugebauer, M.: 1995, *Adv. Space Res.* **16**, 85
Pneuman, G. W.: 1972, *Solar Phys.* **23**, 223
Schmidt, W. K. H., Bothmer, V.: 1996, *Adv. Space Res.* **17**, 369
Somov, B.: 1992, *Physical Processes in Solar Flares*, Kluwer Academic Publ., Dordrecht, London
Steinolfson, R. S.: 1992, *J. Geophys. Res.* **97**, 10811
Strachan, L., Jr.: 1990, *Measurements of Outflow velocities in the Solar corona*, PhD Thesis, Harvard University
Verneta, A. I., Antonucci, E., Marocchi, D.: 1994, *Space Sci. Rev.* **70**, 299

Wang, Y.M., Sheeley, N. R., Jr.: 1990, *Astrophys. J.* **355**, 726
Wang, Y.-M., and Sheeley, N.R. Jr: 1994, *J. Geophys. Res.* **99**, 6597
Wang, A.-H., Wu, S.-T., Suess, S.-T., Poletto, G.: 1995, *Solar Phys.* **161**, 365
Wilson, D. C.: 1977, *The 3-D Solar Corona: a Coronal Streamer*, Ph. D. Thesis, University of Colorado, Boulder
Wu, S.-T., Wang, A.-H.: 1991, *Adv. Space Res.* **11**, 187